Influence of the Stiffness Modulus and Volume Fraction of Inclusions on Compressive Strength of Concrete

Available online at www.sciencedirect.com

ScienceDirect

Procedia Engineering 171 (2017) 760 – 767

Procedia Engineering

www.elsevier.com/locate/procedia

Sustainable Civil Engineering Structures and Construction Materials, SCESCM 2016

Influence of the stiffness modulus and volume fraction of inclusions on compressive strength of concrete

Han Ay Lie[a,*], Buntara Shently Gan[b], Benny Suryanto[c], Yulita Arni Priastiwi[d]

[a]*Civil Engineering Department, Diponegoro University, Semarang, Indonesia*
[b]*Department of Architecture, College of Engineering, Nihon University, Koriyama, Japan*
[c]*School of Energy, Geoscience, Infrastructure and Society, Heriot Watt University, Edinburgh, UK*
[d]*Structural and Material Laboratory, Diponegoro University, Semarang, Indonesia*

Abstract

The stiffness differences between aggregate and mortar matrix in concrete create stress concentration at their interface transition zones. Studies on 100 mm cubes with different volume and shape of inclusions, resembling aggregate particles within the concrete, suggested that it is always in this transition zone that cracks initiate. Further detailed finite element analysis brought to light that especially the mortar nodes in principal tension - compressive stresses were most vulnerable to premature failure. The study also suggested that as the relative stiffness between the inclusion and the surrounding mortar increases, the stress concentration problem increases, resulting in premature cracking and lower compressive strength, when compared to the specimens with more homogeneous stiffness profile. This study aims to investigate in more details the influence of inclusion volume fraction, compressive strength and stiffness modulus on the compressive strength of 100×100×50 mm3 prisms. The inclusions were in cylindrical shape and made of mortar with a compressive strength ranging from approximately 20 MPa to 50 MPa; the matrix was also made of mortar but with a constant compressive strength of approximately 29 MPa. It is found that the compressive strength and initial stiffness of the concrete prisms are directly related to the volume fraction and compressive strength of the inclusions. Finite element analysis is conducted to investigate the influence of the relative strength of inclusion to the surrounding mortar.

Peer-review under responsibility of the organizing committee of SCESCM 2016.

Keywords: inclusion volume fraction; inclusion strength ratio; compressive strength.

* Corresponding author. Tel.: +62-811288313; fax: +62-24-76480727.
E-mail address: hanaylie@hccnet.nl

Peer-review under responsibility of the organizing committee of SCESCM 2016.
doi:10.1016/j.proeng.2017.01.444

1. Introduction

Extensive research work has been conducted to study the influence of aggregate inclusions on the mechanical behavior of mortar and concrete [1-6]. In these studies, the aggregate inclusions were much stronger and stiffer than the surrounding mortar matrix. As a result, when the mortar/concrete specimens were tested to failure, the inclusions remained elastic although the surrounding mortar exhibited highly nonlinear behavior. It was concluded as the inclusion volume fraction is increased, the initial stiffness increases and the compressive strength decreases. The reduction in compressive strength is likely attributed to the weak interfacial transition zone (ITZ) between the aggregate inclusions and the surrounding matrix. Apart from the volumetric ratio, the compressive strength and stress-strain response of the mortar/concrete specimens were found to be influenced by the geometry and configuration of the inclusions, the presence of sharp angles in the direction of loading, the number of inclusions and their distance. Other influencing factors include the absorption rate, surface roughness and material homogeneity of the inclusions. Apart from the study high strength inclusions, work has also been conducted on low strength inclusions such as in a soil mixture [7, 8] and in concrete using synthetic inclusions [9].

This study aims to study the effect of compressive strength and volume fraction of inclusions on the overall compressive strength and elastic modulus of concrete. The inclusions were cylindrical and core drilled from mortar slabs. The 28 days compressive strengths of the inclusions are presented in Table 1, together with the corresponding strengths at 56 days and their relative strengths to that of the surrounding mortar which has a cylinder compressive strength of 29.16 MPa at 56 days.

Table 1. Inclusion cylinder compressive strength

Testing age	Cylinder Compressive Strength (MPa)				
	A1	A2	A3	A4	A5
28 days	22.94	28.89	35.71	39.97	46.06
56 days	23.95	30.11	36.24	41.63	46.80
Strength ratio to mortar	0.82	1.03	1.24	1.43	1.60

This study also investigates the response of concrete as a composite material containing a mixture of aggregate inclusion and mortar. In theory, the behavior of a composite material can be approximated by the parallel (Voigt, constant-strain), series (Reuss, constant-stress), Hirsch and Counto model [10] using the following relationships:

Parallel model: $$E_s = V_a E_a + V_m E_m \quad (1)$$

Series model: $$\frac{1}{E_s} = \frac{V_a}{E_a} + \frac{V_m}{E_m} \quad (2)$$

Hirsch model: $$\frac{1}{E_s} = x\frac{1}{(V_a E_a + V_m E_m)} + (1-x)\left(\frac{V_a}{E_a} + \frac{V_m}{E_m}\right) \quad (3)$$

Counto model: $$\frac{1}{E_s} = \frac{1-\sqrt{V_a}}{E_m} + \frac{\sqrt{V_a}}{(1-\sqrt{V_a})E_m + E_a\sqrt{V_a}} \quad (4)$$

Where E and V represent the elastic modulus and volume fraction; the subscripts s, a and m stand for the specimen, inclusion and mortar, respectively; x and $(1-x)$ are the relative proportions corresponding to the upper and lower bound solutions for elastic materials, customary taken as 0.5 for concrete. It should be noted that the first two models are only a simple approximate as concrete does not exhibit either constant stress or strain even under uniform loading. The Hirsch model, which is a combination of the parallel and the series models, does not provide accurate predictions for soft inclusions. For example, when the aggregate stiffness approaches zero ($E_a = 0$), this would result in zero composite stiffness (e.g. $E_s = 0$) which is incorrect. The Counto model (Eq. 4) therefore appears to be the most accurate model and is useful for this study. The computed composite elastic modulus will be compared to experimental data to gauge the accuracy.

2. Experimental work

The work involved the testing of 100 × 100 × 50 (depth) mm concrete prisms with one single cylindrical inclusion aligned vertically at the center of the square surface. Two test parameters were investigated: inclusion volume fraction and inclusion compressive strength. Four inclusion diameters, 11.7, 20.6, 29.7 and 45.7 mm were prepared, resulting in a volume fraction V_a of 0.01, 0.03, 0.07 and 0.16. Control (mortar only) specimens were also produced representing a zero inclusion volume fraction. For every case, eight specimens were prepared to result in six valid data. The compressive strengths provided in Table 1 were used as the basis for the second parameter.

The specimens were prepared in two stages. The first stage involved the preparation of the inclusions and for this purpose, aggregate inclusions were core drilled from 70 mm thick mortar plates using a diamond core drill. The cylindrical core was then made in a saturated surface dry condition and positioned at the center of 100 × 100 × 50 mm five gang plywood molds (see Fig. 1). The mold had a 5 mm acrylic lid in order to secure the cores in place during casting. This vertical configuration was done to minimize the bleeding effect that could weaken the interface between the cylindrical inclusion and the surrounding mortar.

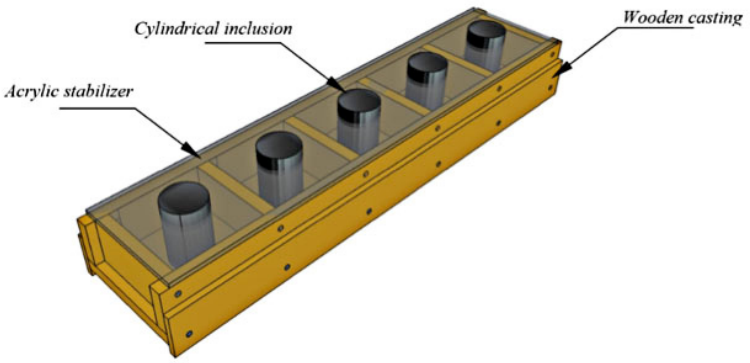

Fig. 1. Cylindrical inclusions placed at the center of a five gang plywood mold.

The second stage involved the mixing and pouring of mortar. Compaction was performed using a vibration table for a period of 30 seconds. The specimens were then submerged in water for 28 days and dried. The top surface of the specimen was made flush by cutting part of the inclusion that protruded 20 mm. The specimens were given label as A_{ij}, with *i* representing the inclusion strength ratio and *j* for the inclusion diameter such as 11, 20, 29 and 45.

The testing surfaces were further leveled, two 100 μm Teflon layers separated by bearing grease were placed on the top and on the bottom face of the specimen to prevent the loading platen's confinement on the specimen. A uniform compression load was applied to each specimen at a rate of 800 N/sec. Four linear variable displacement transducers (LVDTs) with a sensitivity of 2000×10^{-6} strain/mm and a load cell with a capacity of 1000 kN were used to record the load, which was applied incrementally, and the corresponding displacements. Each test specimen was monitored visually using a high definition digital camera to observe the initiation and propagation of cracks under monotonic loading.

3. Test Results

3.1. Compressive strength

Fig. 2 shows the relationship of the inclusion volume fraction for a range of inclusion strengths ratios. It can be seen that an increase in inclusion volume fraction resulted in a decrease in the specimen's load carrying capacity. The behavior followed a linear pattern and all specimens exhibited lower compressive strengths when compared to the control (mortar only) specimen. With regards to the effects of inclusion compressive strength, it appears that the

lower the strength ratio, the more pronounced the reduction in the specimen's capacity relative to that of the control specimen. A1 specimens exhibited an almost identical pattern to A2 specimens, which can be seen from comparable gradients of the plots presented in Fig. 2. This indicates that when the compressive strength ratio is close to unity, it has only minor influence on the reduction rate in compressive strength with increasing inclusion content.

To better analyze the influence of inclusion strength ratio, the load carrying capacity of specimens were plotted against this variable, for every inclusion volume fraction variation. The results are presented in Fig. 3.

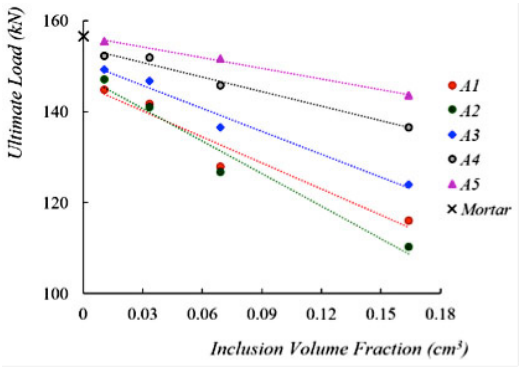

Fig. 2. Influence of inclusion volume fraction on compressive strength

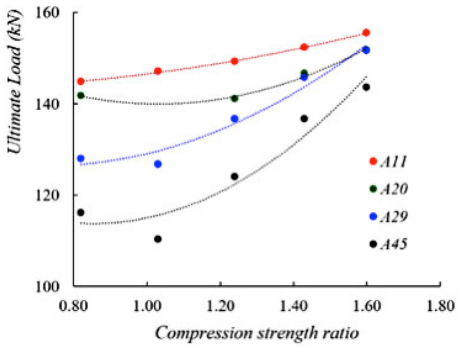

Fig. 3. Influence of strength ratio on compressive strength

The behavior was best described by a quadratic convex path. For all inclusion volume fractions, an increase in compressive strength ratio has a positive influence on the compressive strength of the bulk composite. Larger inclusion volume fractions were more sensitive to strength degradation, which can be seen from the patterns of curves A_{11}. A_{20}, A_{29} and A_{45}. The 0.8 volume fraction resulted from the 11.7 mm inclusion had the most moderate curve's tangent.

3.2. Initial Failure and Crack Propagation

The control (mortar only) specimen failed due to tensile strains in the direction perpendicular to the line of loading, resulting in a columnar pattern (Fig. 4a). For specimens with inclusions, two modes of failure were observed: a columnar pattern with crack passing through the inclusion (Fig. 4b) and a columnar pattern with crack passing around the inclusion due to interface debonding (Fig. 4c).

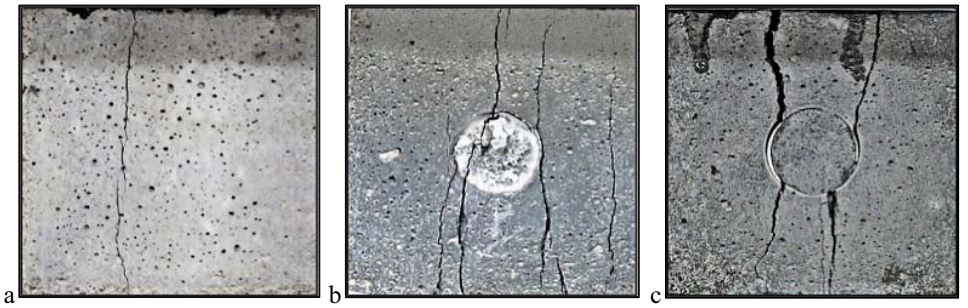

Fig. 4. (a) mortar specimen cracking; (b) cracking in the inclusion; (c) columnar and interface debonding

Cracking in the inclusions was only detected for compressive strength ratios lower than 1.0 (A1 series). In this series, it was found that cracks formed vertically and some of them passed through the cylindrical inclusion (see Fig. 4b). In specimens with larger compressive strengths ratio (A3 to A5 series), the same vertical crack formation was observed. However, it was found that cracks propagated around the cylindrical inclusion along the inclusion/matrix interface, creating an en-echelon formation (Fig. 5a) as explained by van Mier in 1997 [11].

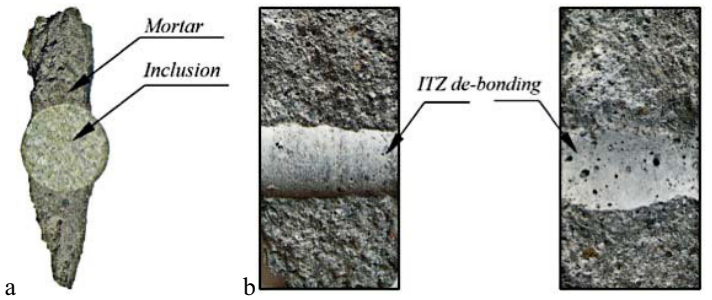

Fig. 5. (a) En-echelon formations; (b) ITZ tension debonding failure surfaces

Close observation of the cracked surface revealed that no mortar fragments were detected in the failure surface (Fig. 5b), indicating ITZ tension debonding behavior. The specimens with a strength ratio of 1.0 (A2 series) exhibited a combination of the two failure behaviors.

The initial cracking was observed visually, from digital recordings. It was observed that regardless of the strength ratios and the volume fraction, cracking was always initiated in the mortar matrix (Fig. 6a and 6b). In A1 series specimen with a strength ratio of 0.8, it was observed that the cracks rapidly proliferated vertically and passed through the inclusion. In A3 to A5 series specimens with strength ratios greater than unity, it was found that the cracks propagated in a straight line and deviated into the interface in tension. In A2 series specimen with a strength ratio of 1.0, an amalgamation of behavior was noted. This particular case was distinguished by an almost identical compressive strength between the mortar matrix and the inclusion.

Since all cracks were initiated in the mortar, it can be concluded that a good bond within the interface is present. This leading to the assumption correctness that the test specimens were a composite material. Also, this finding contradicts the research on diorite inclusions with identical volume fraction [5] where the crack was found always to initiate at the ITZ. Compared to aggregate inclusions, a better bond between mortar inclusions and the surrounding mortar exist.

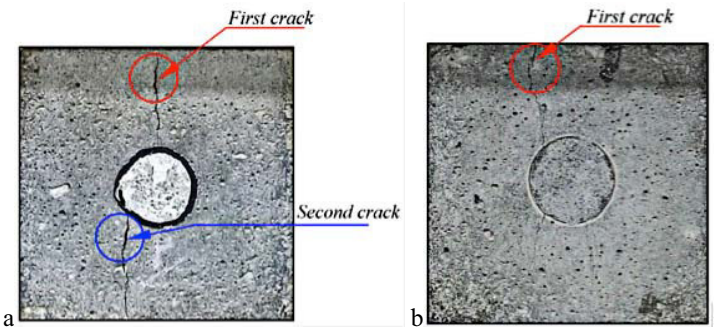

Fig. 6. (a) Initial cracking for strength ratio of 0.8; (b) Initial cracking for strength ratios larger than 0.8

3.3. Initial stiffness modulus

Fig. 7 illustrates the predicted initial stiffness moduli as derived from the Counto equation, plotted together with the observed values determined from the specimen's stress-strain relationship. The Young's modulus of the mortar matrix and inclusions were determined from the cylinder compressive strength in accordance with the *fib* Model Code 2010 [12]. The experimental data are in good agreement with the values as predicted by the Counto equation.

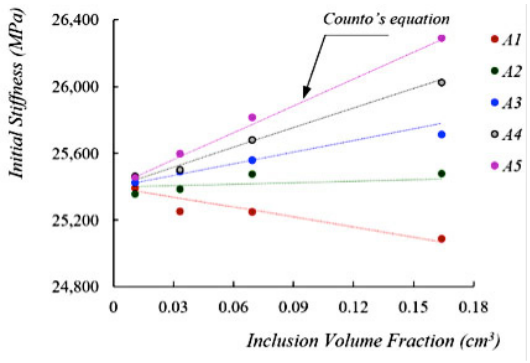

Fig. 7. Initial Stiffness modulus as a function of Volume fraction

4. Analysis and Discussions

4.1. Compressive strength

The reduction in compressive strength with increasing inclusion volume fraction for all strength ratios is thought to originate from the presence of the ITZ. The initial cracking in the mortar suggests that the tensile strength of the interface exceeded the mortar's tensile capacity, yet a perfectly full-bond was not achieved. This conclusion is supported by the 6% to 30% load carrying capacity reduction between the mortar only specimen and the specimen incorporating inclusion with similar strength (1.0 strength ratio). The higher the inclusion volume fraction, the larger the strength reduction. The stresses induced by the load were not uniformly distributed between the mortar matrix and inclusions due to the imperfect ITZ bond. The width of the mortar-strip adjacent to the inclusion is heavily influenced the resulting maximum stresses. These high-stress concentrations, in turn, led to premature cracking of mortar. The result of finite element analysis comparing the stresses in a mortar strip specimen nearby a hole (weak inclusion), inclusion with a perfect bond and no inclusion are shown in Fig 7. The stresses in the direction of the z-z axis are plotted against the nodal coordinates of the mortar strip. In the analysis simulating the effect of inclusion, it

was assumed that the strength ratio is 1.6, and the inclusion is perfectly bonded to the mortar. A similar approach was conducted by [13], validating the finite element results to the iBEM readings.

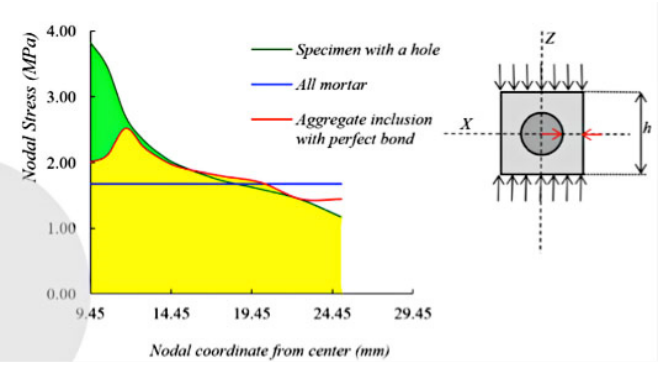

Fig. 8. Stress concentration in the ITZ

The blue line shows the theoretical stresses for the mortar only specimen, the green line stands for the specimen with a hole and the red line represents the analysis case with an inclusion perfectly bonded to the surrounding matrix. The analysis results show that when an inclusion with a perfect bond is present, the stress concentrations in the vicinity of the ITZ are drastically reduced. If the volume fraction increases, the remaining mortar strip will decrease, resulting in a significant escalation in stresses. The true behavior would lay between the two lines, explaining the better load carrying capacity for the inclusion with relatively higher strength ratios. This analysis also supports the fact that for a constant inclusion volume fraction, the higher stress ratios resulted in a better performance in compression. Fig. 8 also implies that for high volume fractions, eq. larger sized inclusions, the low strength ratio has a more pronounced effect on the load carrying capacity. For the larger inclusion volume fraction, the ITZ surface area also increases, resulting in an additional negative effect on the overall specimen behavior.

4.2. Cracking behavior and initial stiffness modulus

The crack propagation is strongly affected by the inclusion strength ratio, but is less influenced by the volume fraction. When the strength ratio is smaller than 1.0, the crack propagation will follow a pattern as if the specimen was homogeneous. No deviation from the columnar path was detected. For a strength ratio larger than 1.0, the cracks propagated through the ITZ in tension, following an en-echelon shear flow. For a strength ratio equal 1.0, a combination of both failure modes occur. When the inclusions have a stronger bond in tension to the surrounding mortar than the mortar matrix tensile capacity, the crack will initiate in the mortar matrix. For aggregate inclusions, the ITZ bond is weaker, first cracking always takes place in the ITZ. However, even for mortar inclusions, the ITZ bond is imperfect, concluded from the reduction in compression strength between the mortar only specimen and the specimen with an equal strength inclusion (strength ratio = 1.0). The finite element models constructed by Wu and Wong [8] using low and high strength inclusions, and the study of iron inclusions [6] underlined these findings.

The evaluation on the initial stiffness revealed that for specimens with an inclusion strength ratio lower than 1.0, the stiffness decreases with increasing inclusion volume fraction. For a 1.0 ratio, the path follows an almost horizontal line, while for ratios larger than 1.0, an enhancement in stiffness is observed. While an increase in inclusion volume fraction always decreases the compressive strength, it may increase the initial stiffness as in a case when the strength ratio is larger than 1.0. The initial stiffness ratio directly related to the compressive strength by the *fib* and the majority of standards is, therefore, incorrect. The approach of Counto provides a better illustration of the stiffness behavior of an inclusion specimen. These findings were also underlined by previous studies [1, 14−15]. The study of Le Roy et al. [14] investigated the inclusion size effect in lightweight concretes. Their research work suggested to asses a physical model rather than an empirical one through, for example, using the Hashin-Shtrikman bounds to approximate the Young's modulus.

5. Conclusions

In a nutshell, it is concluded that a lower inclusion volume fraction, thus smaller inclusions, will lead to a better load carrying capacity regardless of the quality of inclusions. When dealing with larger volume of inclusions, a better performance will be obtained when the inclusions are stronger than the surrounding mortar matrix. When calculating the initial stiffness, the laboratory results obtained support the notion that the stiffness is not only related to the compressive strength. The mathematical models proposed by Counto and Hashin-Shtrikman were proven to provide more accurate predictions of the Young's modulus of concrete.

References

[1] H. Beushausen, T. Dittmer, The influence of aggregate type on the strength and elastic modulus of high strength concrete, Construction and Building Materials, 74, (2015), 132-139.
[2] A. L. Han, B. S. Gan, R. Yuniarto, A. Yesica, R. N. Editia, Inclusion-to-specimen volume ratio Influence on the Strength and Stiffness Behaviors of Concrete: an Experimental Study, in press, Applied Mechanics and Material, Trans Tech Publications, 845, (2016), 113-118.
[3] A.L. Han, B. S. Gan, and Y. Setiawan, The Aggregate Multi-inclusion Interaction and Interface Influence on the Compression Behavior of Concrete, in: S. Saha, Y. X. Zhang (Eds), Implementing Innovative Ideas in Structural Engineering and Project Management, ISEC Press, 2015. 695-700.
[4] A. L. Han, I. Nurhuda, Y. Setiawan, The Effect of Aggregate Shape and Configuration to the Concrete Behavior", Smart Science, Taylor and Francis online, 2-2, (2014a), 85-90.
[5] A. L. Han, B. S. Gan, Y. Setiawan, The influence of single inclusions to the crack initiation, propagation and compression strength of mortar, Procedia Engineering, 95,(2014b), 376-385.
[6] Y. Kan, K. Pei, C. Chang, 2004, Strength and Fracture Toughness of Heavy Concrete with Various Iron Aggregate Inclusions, Nuclear Engineering and Design, 228-1-3, (2004), 119-127.
[7] G. van Lysebetten , A. Vervoort, J. Maertens, N. Huybrechts, Discrete element modeling for the study of the effect of soft inclusions on the behavior of soil mix material, Computers and Geotechnics, 55, (2014), 342-351.
[8] Z. Wu, L. N. Y. Wong, Modeling cracking behavior of rock mass containing inclusions using the enriched numerical manifold method, Engineering Geology, 162, (2013), 1-13.
[9] J. Lv, T. Zhou, Q. Du, H. Wu, Effects of rubber particles on mechanical properties of lightweight aggregate concrete, Construction and Building Materials, 91, (2015), 145-149.
[10] U. J. Counto, The effect of the elastic modulus of the aggregate on the elastic modulus, creep and creep recovery of concrete, Magazine of Concrete Research, 16-48, (1964), 129-138.
[11] J.G.M. van Mier, Failure of concrete under uniaxial compression: an overview, in: H. Mihashi, K. Rokugo (Eds.), Fracture Mechanics of Concrete Structures 3, AEDIFICATIO, Freiburg, 1998, pp. 1169–1182.
[12] fib Model Code for Concrete Structures 2010, Ernst & Sohn, Berlin, 2013.
[13] G. Song, L. Wang, L. Deng, H. M. Yin, Mechanical characterization and inclusion based boundary element modeling of lightweight concrete containing foam particles, Mechanics of Materials, 91-1, (2015), 208-225.
[14] R. Le Roy, E. Parant, C. Boulay, Taking into account the inclusions' size in lightweight concrete compressive strength prediction, Cement and Concrete Research, 35-4, (2005), 770-775.
[15] E. J. Garboczi, J. G. Berryman, Elastic Moduli of Material Containing Composite Inclusions: Effective Medium Theory and Finite Element Computations, Mechanics of Materials, 33-3, (2001), 455-470.